Journal of Molecular Structure, 189 (1988) 65-80
Elsevier Science Publishers B.V., Amsterdam — Printed in The Netherlands

CONFORMATIONAL ASPECTS OF MALIC ACID: A MULTIDISCIPLINARY APPROACH*

PIETER F.W. STOUTEN, BAS R. LEEFLANG, BOUKE P. VAN EIJCK and JAN KROON

Laboratorium voor Kristal- en Structuurchemie, Vakgroep Algemene Chemie, Rijksuniversiteit, Padualaan 8, 3584 CH Utrecht (The Netherlands)

JAN-REMT MELLEMA

Analytical Research and Development Laboratories, Organon International B.V., P.O. Box 20, 5340 BH Oss (The Netherlands)

(Received 14 January 1988)

ABSTRACT

Malic acid molecules can adopt three different staggered conformations of minimum energy with respect to rotation around the central C-C bond: *gauche*$^-$ (g−), *trans* (t) and *gauche*$^+$ (g+). The conformational behaviour of the acid and of its dissociated forms has been studied by means of NMR experiments and Molecular Dynamics simulations and the results are compared with a statistical analysis of crystal structures and with Molecular Mechanics calculations.

Specific coupling constants for all three ionization states were determined. Coupling constants of the three staggered rotamers were calculated and by comparison with the specific coupling constants of each ionization state rotamer populations were determined.

Observed and calculated populations are similar, although the *gauche*$^-$ population resulting from the NMR experiment is significantly higher than predicted by the other methods. All techniques indicate that *gauche*$^+$ is the minor conformer of the neutral molecule. It is also shown that water-acid interactions play a very important role in describing the conformational behaviour of malic acid properly.

INTRODUCTION

Malic acid is, in its ionized form, one of the compounds that constitute the last stage of the citric acid cycle. Until now two crystal modifications of the racemic compound have been encountered, whose structures have been solved by X-ray diffraction [1,2]. Mariano and Gil have carried out NMR measurements on the neutral and doubly charged species [3]. In order to investigate its molecular conformation in more detail energy minimizations of the isolated malic acid molecule have also been carried out [4]. We endeavoured to study

*Dedicated to Professor D. J. Millen on the occasion of his retirement.

0022-2860/88/$03.50

the behaviour of malic acid in aqueous solution by nuclear magnetic resonance (NMR) in a more detailed fashion and by molecular dynamics simulations (MD). Attention was focussed on rotation about the central C–C bond. At room temperature there is fast rotation about this bond, but of course there is a distinct preference for staggered conformations. We shall assume in the following that in the system under consideration every malic acid molecule will adopt approximately staggered conformations only. These conformations need not be ideally staggered (where the C–C–C–C torsion angle would be −60, 60 or 180°). L (2S) Malic acid is depicted in its *trans* form in Fig. 1 together with the atom numbering. Figure 2 shows the Newman projections of the three rotamers where the nomenclature refers to the C–C–C–C torsion angle.

Molecular dynamics simulations are widely used nowadays to investigate properties of liquids, solutions and crystals. The method can be used on its own, for example to obtain all kinds of radial and angular distributions that can hardly be assessed through experiments on real liquids [5]. It can be used in combination with NMR to determine the structure of proteins in aqueous solutions [6] or even to refine crystal structures of proteins [7]. We did MD simulations of L-malic acid in water (MD_{aq}) to obtain geometrical and energetical data on all three rotamers. Of course, molecular mechanics (MM) energy minimizations could also provide some knowledge about geometries and energies. It is, however, a limited technique because firstly one studies isolated (gas phase) molecules and secondly it is impossible to leave local energy min-

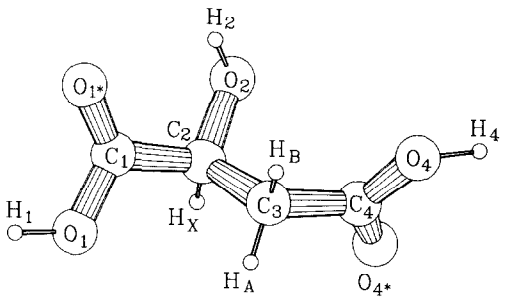

Fig. 1. L-Malic acid in its *trans* conformation, showing atom numbering.

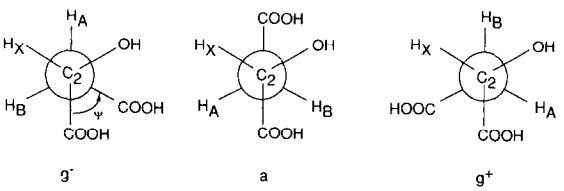

Fig. 2. Newman projections of the three staggered malic acid rotamers.

ima once entered. MD does not have these drawbacks: it is perfectly capable of incorporating many solvent (water) molecules, making it possible to mimic in vitro or in vivo conditions, and the simulated molecules have no problems climbing barriers in the order of kT. Moreover the newest developments provide an elegant means to calculate ΔG differences, e.g. between different conformations [8].

NMR is a commonly used technique in conformational analysis. In the case of malic acid useful information can be obtained from vicinal (or three-bond) coupling. Malic acid contains three aliphatic protons henceforth referred to as H_A, H_B and H_X. H_A and H_B are attached to carbon C_3 and H_X to the neighbouring carbon C_2 (see Fig. 1). These three coupled spins (protons) give rise to a proton spectrum displaying a typical ABX-pattern. Mariano and Gil [3] have studied malic acid and its di-sodium salt by NMR and interpreted the results from the ABX-pattern analysis in terms of rotamer populations under the assumption that the former does not dissociate and the latter does not associate. We thought this too crude an approach and thus determined coupling constants at several pH values. Because association and dissociation are fast on the NMR time scale, the observed coupling constants at any pH are weighted averages of specific coupling constants of all three ionization states. Since internal rotation is also fast, these specific coupling constants, in turn, are population weighted averages of coupling constants of all three rotamers. From the measurements at different pH values the specific coupling constants can be derived. Subsequently the populations for every individual ionization state can be calculated and compared with the results from the MD_{aq} simulations, MM calculations and with crystal structure statistics.

MOLECULAR DYNAMICS SIMULATIONS

Neutral L-malic acid dissolved in water was simulated on the Cyber 205 of the Amsterdam Academic Computer Center (SARA) using the GROMOS simulation package [9]. For water the SPC potential, which allows no intramolecular degree of freedom, was used [10]. For malic acid we employed the standard GROMOS potential function, but in order to account for the well known tendency of the O_1–C_1–C_2–O_2–H_2 part of glycolic acid groups to be planar, extra torsion potentials derived from ab-initio data on glycolic acid were added [11,12]. The complete potential function is detailed in the Appendix. All bond lengths were kept fixed, which saves considerable amounts of computing time and does not affect the properties of the system [13]. For all three rotamers independent simulations were carried out for a system consisting of 1 malic acid molecule and 216 water molecules in a rectangular box with periodic boundary conditions using a cut-off for the potential of 7 Å. This cut-off radius is applied to atom groups with no net charge, the so-called charge groups. In our case every water molecule and the COOH, CHOH and CH_2 groups of malic acid make up charge groups. The list of interacting charge

group pairs was updated every 5 time steps. A time step of 1 fs was employed and relevant data were sampled during a period of at least 10 ps after an initial equilibration period of at least 5 ps. The system was loosely coupled to a pressure bath of $p=1$ atm. and a temperature bath of $T=298$ K with coupling time constants of 0.5 and 0.1 ps respectively [5,14]. In all cases the volume did not deviate much from the average value of 6.8 nm^3 corresponding to a concentration of 0.24 mol l^{-1} and a density of 0.98 kg l^{-1}. In all three simulations the average temperature was about 302 K. Even in our rather short simulations several transitions between the *trans* and *gauche*$^+$ conformers occurred, so we had to run several independent simulations in order to obtain sufficient data. No transitions to or from the *gauche*$^-$ conformer were observed, which leads us to the conclusion that the barrier between *trans* and *gauche*$^+$ is much lower than the *gauche*$^-$/*trans* and *gauche*$^-$/*gauche*$^+$ barriers. This is in agreement with the MM calculations [4].

The properties of interest here are the differences in (free) energy between the different conformers. Of course one must consider the energetic contributions of the complete system, including all water molecules, but the very long simulations, at least 400 ps per conformer, that are necessary to reduce the noise caused by the water–water interactions to about 3 kJ mol^{-1} of malic acid are not feasible. If one assumes that for all three malic acid conformers the water molecules are arranged in a similar fashion, then the differences in energy due to acid–acid and acid–water interactions (denoted E(acid, total)) which can be calculated more accurately, will be very close to the differences in the total energy that would result from longer simulations. Mean energies and temperature together with root mean square (RMS) deviations are detailed in Table 1. For comparison relative MM energies are also given [4]. Standard deviations in the mean total energy and potential energy were calculated using the following equation, derived by Berendsen et al. for time correlated properties [15]:

$$\sigma(\langle E\rangle)=\mathrm{RMS}(E)\times((1+2\tau)/n)^{1/2} \quad (1)$$

TABLE 1

Energies[a] (in kJ mol^{-1}) of the three conformers resulting from the MD simulations (MM energies are given for comparison)

	E(tot)	E(pot)	E(acid, total)	E(acid, intra)	Temperature (K)	MM
g−	−7446(38)	−9102(69)	−233(16)	−12.3(6.0)	302.3(8.4)	0.0
t	−7440(35)	−9098(64)	−232(18)	−26.0(6.1)	302.6(8.5)	4.4
g+	−7461(44)	−9113(61)	−217(20)	−22.1(4.8)	301.6(8.3)	7.5

[a]RMS values in parentheses.

where n is the total number of dependent observations (time steps) and τ the correlation length of the considered property. For the potential energy we found $\tau = 420$ time steps and $\sigma(\langle E \rangle) = 16$–$18$ kJ mol^{-1}. For the total energy $\tau = 822$ and $\sigma(\langle E \rangle) = 16$–$20$ were found. As expected these standard deviations are too large to determine reliable rotamer populations. We did not calculate correlation lengths for the intramolecular energy of malic acid E(acid, intra) and E(acid, total) but the standard deviations in the mean value of these energies are expected to be in the range of 2–3 and 6–7 kJ mol^{-1} respectively. The E(acid, total) values show clearly that *gauche*$^+$ is the least populated rotamer, but one cannot decide whether *gauche*$^-$ or *trans* is predominant. It is noteworthy that *gauche*$^-$ has by far the highest intramolecular energy, but that this is more than compensated for by favourable acid–water interactions. In order to obtain more accurate results longer MD simulations or stochastic dynamics simulations are necessary. An even better approach is to calculate free energy differences using MD techniques [8] because firstly they are directly related to populations and secondly they can be determined more precisely than energies. These calculations are in progress.

NMR EXPERIMENT

Proton spectra of a solution of 0.5 M non-deuterated malic acid in D_2O were measured on a Bruker WP200 and a Bruker AM360 at room temperature at several pH values ranging from 0.3 to 13.5. The pH was varied with NaOD and D_2SO_4 solutions. Coupling constants were determined in standard iterative process. Figures 3 and 4 show spectra at pH = 6.5 and pH = 2.65 respectively. The left-most peak is due to HOD. Next to this peak the double doublet of the X-proton is found at 4.3 ppm. The A and B-protons are in the high-field region of the spectrum. An assignment of these signals was made by assuming that the *trans* rotamer is dominant when both carboxyl groups are charged, as is the case for 95% of the molecules at pH = 6.5. Owing to the highly repulsive coulombic interaction this is a valid assumption. In the *trans* rotamer the torsion angle between H_X and H_B is close to 180°, while the torsion angle between H_X and H_A is approximately −60°. According to the Karplus relationship between the torsion angle and the vicinal coupling constant, the coupling between H_X and H_B should be significantly larger than the coupling between H_X and H_A [16]. The multiplet at 2.4 ppm, having a vicinal coupling of nearly 10 Hz, was therefore assigned to proton B. The signal at 2.7 ppm, having a coupling of about 3 Hz, was assigned to proton A. At pH = 2.65, when most malic acid molecules are uncharged, proton B shifts downfield close to proton A (Fig. 4), so obviously the difference in shielding of the A- and B-protons decreases with decreasing charge.

In order to extract information about the conformational equilibrium from the NMR data, the first step is to obtain coupling constants as a function of

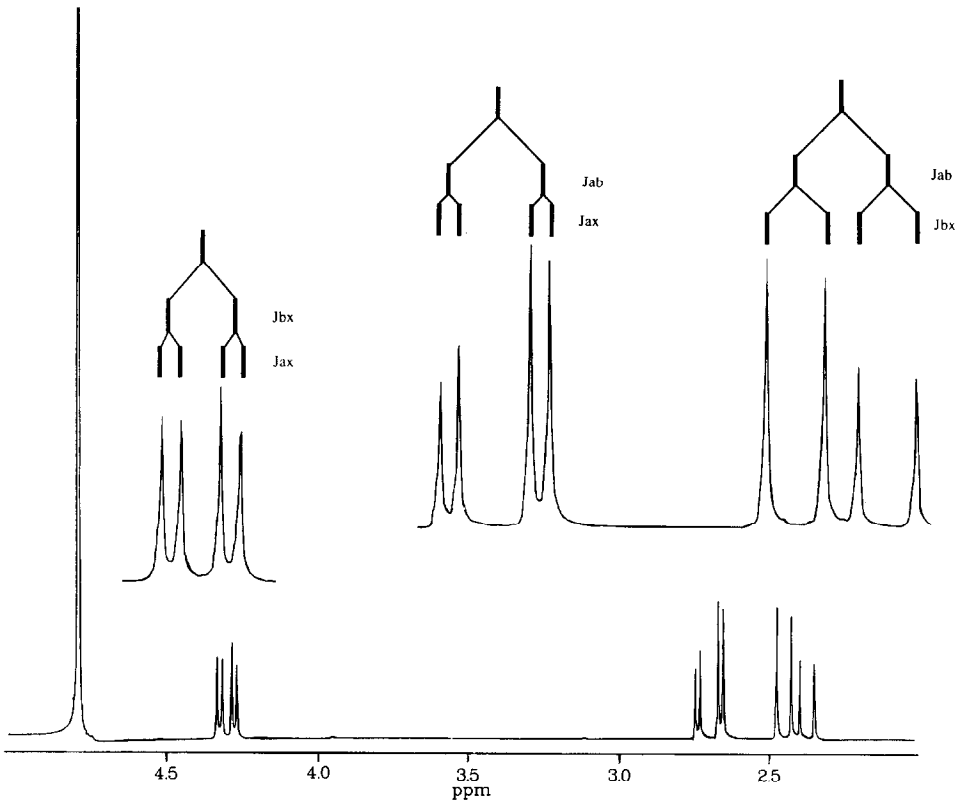

Fig. 3. Proton NMR spectrum of malic acid in D_2O at pH = 6.5.

the ionization state instead of pH. This can be accomplished if the pD and the pK_a values of deuterated malic acid (denoted $pK_1(D)$ and $pK_2(D)$ respectively) are known. For our conventional pH meter with glass electrode the experimental relation pD = pH (meter reading) + ΔpD (where the correction term ΔpD is 0.40 for completely deuterated solutions) can be used throughout the whole pH range [17,18]. Furthermore it has been shown that the correction is very nearly a linear function of the deuterium content of the solution [18]. Assuming complete exchange of all three hydroxyl hydrogen atoms of malic acid the deuterium content is 98.6%. However, even when calculating rotamer populations for contents varying between 97 and 100% the maximum change in any population appears to be only 0.1% absolute. In these calculations the pD correction term as well as differences in pK_a values for deuterated and non-deuterated malic acid were taken into account. $pK_a(D)$ values of malic acid are not tabulated so we estimated them. Lowe and Smith [20] and Glasoe and Long [18] give average ΔpK_a ($= pK_a(D) - pK_a(H)$) values of 0.44 for organic acids. Dahlgren and Long found ΔpK_1 and ΔpK_2 values of 0.46 and 0.42

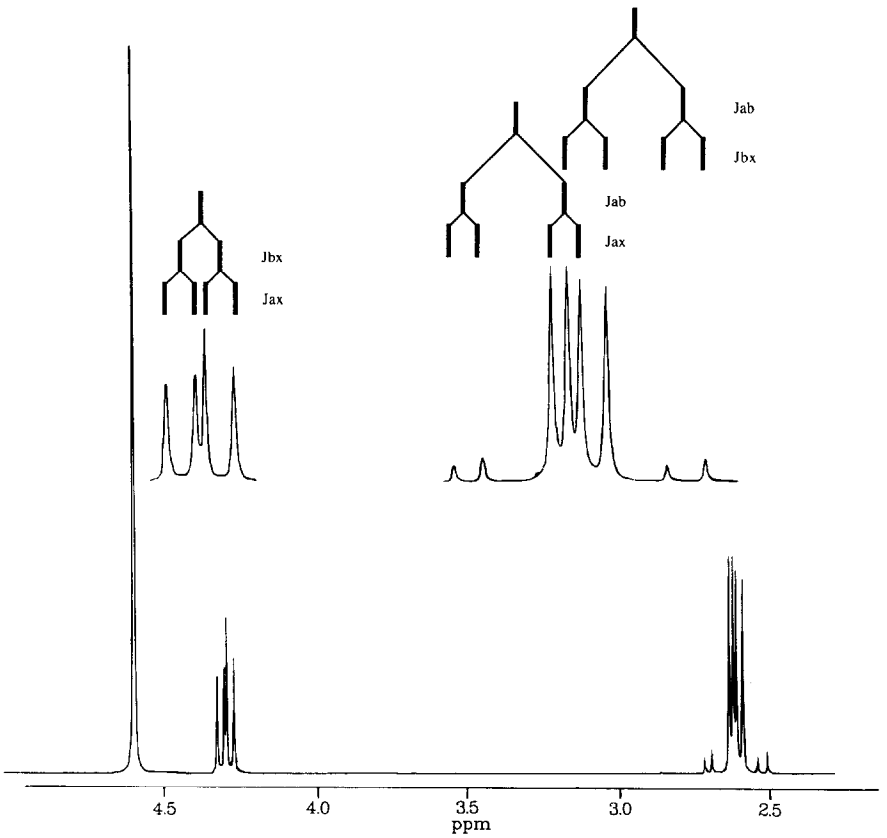

Fig. 4. Proton NMR spectrum of malic acid in D_2O at pH = 2.65.

respectively for fumaric acid [19], which has $pK_a(H)$ values close to those of malic acid and has a similar structure too, so one might assume that these ΔpK_a values are valid in the case of malic acid too. They also give a generalized $\Delta pK_a - pK_a(H)$ relation that holds when no strong intramolecular hydrogen bonding occurs in the conjugate base. The first dissociation constant of fumaric acid (no intra bond possible) is much smaller than the first one of maleic acid (strong intra bond), although they only differ in the *cis/trans* position of two carboxyl groups. The first dissociation constant of malic acid is even smaller indicating that intramolecular hydrogen bonding is no important stabilizing factor in the base. Therefore we applied this relation to malic acid deriving ΔpK_1 and ΔpK_2 values of 0.47 and 0.53. On the basis of these three combinations of ΔpK_a values (0.44/0.44, 0.46/0.42 and 0.47/0.53) and $pK_a(H)$ values of 3.47 and 5.19 [21] we calculated mole fractions of all ionization states (D_2Z, DZ^- and Z^{2-}).

The observed average coupling constants are linear combinations of specific coupling constants and defined as:

$$^3J_\alpha = \sum_{s=D_2Z,\ DZ^-,\ Z^{2-}} f(s)\ ^3J_{\alpha,s} \qquad (2)$$

where α is AX or BX, $^3J_\alpha$ the observed average coupling constant, $f(s)$ the mole fraction of species s and $^3J_{\alpha,s}$ the unknown coupling constant of s. In order to determine the $^3J_{\alpha,s}$ values, the two times nine equations resulting from the pH measurements were solved using standard least squares. Resulting specific coupling constants are given in Table 2, together with those obtained by other authors for H_2Z and Na_2Z solutions. Observed coupling constants and mole fractions averaged over all three ΔpK_a combinations are given in Table 3. Strik-

TABLE 2

Specific coupling constants[a] (in Hz) of all ionization states

s	Present work		Other authors					
	$^3J_{AX,s}$	$^3J_{BX,s}$	Ref. 3		Ref. 22		Ref. 23	
			$^3J_{AX}$	$^3J_{BX}$	$^3J_{AX}$	$^3J_{BX}$	$^3J_{AX}$	$^3J_{BX}$
D_2Z	4.45 (0.09)	6.85 (0.15)	4.2	7.3	4.4	7.0	4.4	7.0
DZ^-	4.07 (0.14)	8.10 (0.24)						
Z^{2-}	3.12 (0.11)	10.03 (0.20)	3.2	9.5	3.1	9.7	2.8	10.3

[a]Estimated standard deviations in parentheses.

TABLE 3

Observed and calculated quantities as a function of pH[a]

Observed				Calculated				
pH	$^3J_{AX}$	$^3J_{BX}$	σ^3J	$^3J_{AX}$	$^3J_{BX}$	$f(D_2Z)$	$f(DZ^-)$	$f(Z^{2-})$
0.30	4.32	6.77	0.09	4.44	6.85	99.9	0.1	0.0
1.71	4.58	6.98	0.08	4.43	6.87	98.5	1.5	0.0
2.65	4.37	7.01	0.07	4.39	7.00	88.2	11.8	0.0
2.96	4.28	7.34	0.08	4.36	7.12	78.5	21.4	0.1
3.55	4.24	7.24	0.06	4.24	7.52	48.2	50.8	1.0
3.91	4.40	7.47	0.06	4.15	7.80	28.4	68.4	3.2
4.52	3.76	8.69	0.06	3.96	8.28	7.9	77.6	14.5
6.50	3.17	9.97	0.06	3.17	9.92	0.0	5.4	94.6
13.50	3.15	9.94	0.10	3.12	10.03	0.0	0.0	100.0

[a]pH is measured pH. $^3J_{AX}$ and $^3J_{BX}$ are the observed and calculated coupling constants in Hz and σ^3J is the standard deviation of the observed coupling constants (equal for $^3J_{AX}$ and $^3J_{BX}$). $f(D_2Z)$, $f(DZ^-)$ and $f(Z^{2-})$ are the calculated mole fractions of the three species.

ing differences between observed and calculated coupling constants are found for intermediate pH values, the maximum being 0.41 Hz. This can be attributed largely to the assumption that all activity coefficients are 1.0. In the case of malic acid it is impossible, however, to tackle the problem of activity adequately. Calculated specific coupling constants of D_2Z and Z^{2-} do not change much, when ionic strength effects are taken into account in an elementary fashion. The largest change is less than half the estimated standard deviation. In the case of DZ^-, however, shifts as large as 0.29 and 0.72 Hz were calculated for $^3J_{AX,DZ^-}$ and $^3J_{BX,DZ^-}$ respectively corresponding with an increase of the calculated *gauche*$^-$ population by 7% and an equal decrease of the *trans* population. This ionic strength problem introduces substantial correlated uncertainties in the mole fractions that make up the least-squares matrix. Consequently the standard deviations given in Table 2 should be regarded as an indication of the relative accuracy of the specific coupling constants.

INTERPRETATION

In order to interpret the data given in Table 2 in terms of populations of the three rotameric forms of every species, the specific coupling constants are regarded as linear combinations of the coupling constants of three minimum energy rotamers:

$$^3J_{\alpha,s} = x^-(s)\ ^3J_\alpha(g-) + x^+(s)\ ^3J_\alpha(g+) + (1 - x^-(s) - x^+(s))\ ^3J_\alpha(t) \qquad (3)$$

where $x^-(s)$ and $x^+(s)$ are the mole fractions of rotamers *gauche*$^-$ and *gauche*$^+$ of species s. Haasnoot et al. have derived an equation to calculate vicinal coupling constants of substituted ethanes as a function of the H–C–C–H torsion angle ϕ [24]. For tri-substituted ethanes such as malic acid they give:

$$^3J(\phi) = 13.22\cos^2(\phi) - 0.99\cos(\phi) + \Sigma\,\Delta\chi_j\{0.87 - 2.46\cos^2(\xi_j\phi + 19.9\,|\Delta\chi_j|)\} \qquad (4)$$

where $\Delta\chi_j$ is the difference in Huggins-electronegativity between substituent S_j and hydrogen (1.3 for OH and 0.4 for COOH [25]), ξ_j is ± 1 depending on the orientation of the substituent, and the summation extends over all three substituents. Projecting the H_X–C_2–C_3–H_β fragment (where β is A or B) along the vector C_2–C_3 and considering substituent S_j on C_2, ξ_j is $+1$ when the projected valency angle between H_X and S_j is approximately $+120°$ (counting clockwise from H_X). ξ values for substituents on C_3 are likewise defined, by projection along the vector C_3–C_2. In Fig. 5 ξ values for AX and BX coupling are shown.

Haasnoot et al. [24] considered coupling constants of 100 tri-substituted ethanes and determined the corresponding torsion angles using MM energy

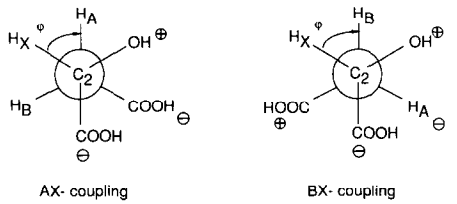

Fig. 5. Definition of orientation coefficients ξ.

minimization procedures. Although they only considered rather rigid structures it must be stressed that in general torsion angles stemming from MM calculations are different from those stemming from MD_{aq} simulations. The latter is a far better model for the system under study by NMR. A further reason they give for employing MM instead of using, for example, crystal data is that hydrogen bonding is thereby ruled out. This, however, is not desirable since hydrogen bonding is of major importance in real systems. Furthermore it is also very possible that intramolecular hydrogen bonds replace the intermolecular ones in the MM calculations (as has been shown to happen in several sugars, such as α-D-glucose, β-D-allose and β-D-digitoxose [4]), which will influence the calculated optimum torsion angles. Despite these disadvantages one must bear in mind that the Haasnoot equation has a far better predictive value than similar ones and its precision, expressed as the root mean square deviation (0.485 Hz), is superior to any hitherto reported.

When one wants to solve eqn. (3) a few problems arise. Firstly when DZ^- is concerned two species should be taken into account, since either O_1 or O_4 can lose a proton. However, because glycolic acid (similar to the C_1–C_2 half of malic acid) has a much higher dissociation constant than acetic acid (similar to the C_3–C_4 half) and in crystal structures of acid salts of malic acid only dissociated C_1-carboxyl groups are found, one can safely assume that only one species has to be considered. Secondly it is implicitly assumed that average and minimum-energy torsion angles are the same for neutral and charged species, which makes the rotamer populations calculated for DZ^- and Z^{2-} somewhat less reliable. Thirdly it is not clear whether one should use torsion angles resulting from MM calculations or MD simulations for calculation of the rotameric coupling constants. If, for all molecules considered by Haasnoot et al., no systematic difference exists between minimum-energy MM torsion angles and average MD_{aq} ones then MD values should be used. If, however, such a difference does exist then MM data are the better choice. Probably the truth will be somewhere in the middle. For both models torsion angles and corresponding coupling constants, calculated with eqn. (4) are given in Table 4. For comparison coupling constants calculated by Mariano and Gil [3] are also given. Haasnoot et al. do not give standard deviations in the parameters and data on correlations, so we varied parameters between "reasonable" values and

TABLE 4

ψ(C-C-C-C) torsion angles (in degrees) and corresponding coupling constants (in Hz) of the three rotamers for different neutral malic acid models
$\phi(H_A\text{-}C\text{-}C\text{-}H_X)=\psi+120°$. $\phi(H_B\text{-}C\text{-}C\text{-}H_X)=\psi$

Rotamer	MM			MDaq			Mariano and Gil	
	ψ	$^3J_{AX}$	$^3J_{BX}$	ψ	$^3J_{AX}$	$^3J_{BX}$	$^3J_{AX}$	$^3J_{BX}$
g−	−60.8	3.99	1.85	−68.7	5.18	1.20	4.8	1.8
t	175.1	1.69	11.23	170.9	1.36	10.88	1.8	14.5
g+	63.7	11.60	3.57	68.4	11.59	2.94	14.5	4.8

TABLE 5

Populations of rotamers and esimated standard deviations in %, based on NMR

	MM torsion angles			MD torsion angles			Mariano and Gil			e.s.d.		
	g−	t	g+	g−	t	g+	g−	t	g+	g−	t	g+
D_2Z	30	49	21	24	55	21	51	42	7	6	3	5
DZ^-	17	63	20	10	67	23				7	4	6
Z^{2-}	1	85	14	0	85	15	37	60	3	8	5	7

TABLE 6

Populations of rotamers in % from MM and MD calculations and observed in crystals[a]

	Crystals				MM			MD_{aq}		
		g−	t	g+	g−	t	g+	g−	t	g+
H_2Z	(2)	0	100	0	82	14	4	60	40	0
HZ^-	(19)	26	74	0						
Z^{2-}	(15)	73	27	0						
Total	(36)	44	56	0						

[a]Numbers of crystal structures involved are given in parentheses.

subsequently estimated standard deviations in the calculated populations. For the population *gauche*$^-$ of Z^{2-} a negative value was calculated when using MD torsion angles, so we recalculated the *gauche*$^+$ and *trans* populations, giving *gauche*$^-$ a fixed value of zero. Differences in the order of 1–7% were observed between the populations calculated on the basis of MM torsion angles and those determined using MD ones. Because of the negatively calculated population *gauche*$^-$ of Z^{2-} when using MD torsion angles, the use of MM torsion angles in eqn. (4) is preferable in our case. Calculated populations and esti-

mated standard deviations (e.s.d.'s) are given in Table 5 together with the results obtained by Mariano and Gil.

In order to compare the NMR, MM and MD results with crystal statistics of malic acid we searched the Cambridge crystallographic database [26] for structures that contained at least one malic acid fragment or its salt. The 36 fragments found were converted into the L-configuration and the distribution of Ψ over the ionization states was determined. The population densities of the rotamers in the simulations were calculated from MD-E(acid, total) and MM energies with neglect of a possible entropy effect. The crystal statistics and calculated populations are detailed in Table 6.

DISCUSSION

The *gauche*$^+$ conformer is not found in crystals and our MD, MM as well as Mariano and Gil's NMR results show that *gauche*$^+$ is the minor species. Our NMR results do not agree quantitatively and even if ionic strength effects are taken into account considerable differences remain between our and Mariano and Gil's results. There may be several reasons for this. Errors could have been introduced in the process of deriving specific coupling constants. The calculated populations for the extreme pH cases (assuming that only D_2Z is present at pH = 0.3 and only Z^{2-} at pH = 13.5) did not differ much, however (the largest change being only 2%). Another reason could be the neglect of β-substitution effects but explicitly including these effects made only a marginal difference (largest change 4%). On the basis of their results Mariano and Gil concluded that the effect of the carboxyl groups could be ignored altogether. Therefore, we calculated populations with electronegativity values of zero for the carboxyl groups, which introduced shifts in the populations up to 8%. It is clear that the influence of the carboxyl groups should be taken into account and Table 5 shows that the influence of torsion angles is also considerable. In this respect Mariano and Gil's simple model fails, whereas Haasnoot's does not. So our results must be regarded more reliable since they are based on a more precise model.

Whatever different results they give, the tendency to decreasing *gauche*$^-$ and *gauche*$^+$ populations with increasing charge is reproduced by both Haasnoot's and Mariano and Gil's models. Furthermore, our NMR results predict *trans* DZ^- to be predominant which is observed in crystals too. In case of crystal structures of the doubly charged species the *gauche*$^-$ conformer is predominant, which does not agree with the NMR results, but this can be attributed to the coordination to cations and other packing forces which have a decisive influence on the conformation. The MM results indicate that *gauche*$^-$ D_2Z is the major species by far, which does not agree with the other results. It has been shown, however, that the *trans* conformer has access to a larger conformational space than *gauche*$^-$ [4], although this cannot account completely for

the large population difference. This shows clearly that acid–water interactions are crucial to describe the rotational behaviour of malic acid in water properly. The MD results agree well with NMR (apart from the *gauche*$^+$) and with crystal statistics.

CONCLUSIONS

We have demonstrated that a useful comparison can be made of the conformational properties of malic acid in the solid, liquid and "computational" phase. Calculated populations are similar, but it should be noted that the interpretation of NMR data heavily depends on the reliability of either Haasnoot's or Mariano and Gil's model. Until now only populations of the neutral and doubly charged species were calculated using NMR data. Although the first and second dissociation constants of malic acid are not very far apart, we have shown that it is possible to obtain data on the singly charged species as well. The MD results look promising and longer simulations and ΔG calculations should provide more reliable populations.

ACKNOWLEDGEMENT

We thank W.F. van Gunsteren for the use of the GROMOS package, G.N. Wagenaars and C. Funke for assistance in the NMR experiments and L.M.J. Kroon-Batenburg for valuable discussions.

APPENDIX: INTERACTION MODEL FOR L-MALIC ACID IN WATER

The interaction model treats all atoms explicitly with the exception of CH and CH_2 groups, which are regarded as united atoms. Polarizability is not taken into account. Partial charges are centered on the nuclei. The model falls apart in so called bonded (intramolecular) and non-bonded interactions.

The non-bonded interaction between atoms i and j is governed by a Lennard-Jones–Coulomb 12-6-1 effective pair potential function:

$$V_{ij} = \frac{C_{12}(i,j)}{r_{ij}^{12}} - \frac{C_6(i,j)}{r_{ij}^{6}} + \frac{q(i) \times q(j)}{4\pi\epsilon_0 r_{ij}} \tag{5}$$

where $C_{12}(i,j)$ and $C_6(i,j)$ respectively are the repulsive and attractive van der Waals' parameters for the atom pair i–j, q_i and q_j the partial charges centered on i and j and r_{ij} is the internuclear distance between i and j. Non-bonded interactions between two atoms belonging to the same molecule and separated by one or two bonds (1–2 and 1–3 interactions) are excluded. 1–5 and higher interactions are governed by the general C_{12}–C_6 atom pair parameters. In order to model rotational behaviour correctly, deviating C_{12}–C_6 parameter values are used for 1–4 interactions that concern CH and CH_2 atoms. Hydroxyl and water

hydrogen atoms (atom types HO and HW) have C_{12} and C_6 values of zero. Partial charges and the atom type definition are given in Table 7. C_{12} and C_6 values are given in Table 8.

Intramolecular geometries are defined in terms of bond lengths, bond angles,

TABLE 7

Partial charges (in |e|) and type definition of malic acid and water atoms

	Name	Type	Charge	Description
Malic acid	H_1, H_3, H_4	HO	0.398	hydroxyl hydrogen
	O_1, O_3, O_4	OA	−0.548	hydroxyl oxygen
	O_{1*}, O_{4*}	O	−0.380	carbonyl oxygen
	C_1, C_4	C	0.530	bare sp^2 carbon
	$C_2(+H_X)$	CH	0.150	methine group
	$C_3(+H_A,H_B)$	CH2	0.000	methylene group
Water	-	OW	−0.820	water oxygen
	-	HW	0.410	water hydrogen

TABLE 8

Van der Waals' C_{12} and C_6 parameters[a]

C_{12}		OA	O	C	CH	CH2	OW
general pairs	OA	1.506					
	O	1.381	0.741				
	C	1.582	1.582	3.374			
	CH	7.293	7.293	15.560	71.756		
	CH2	5.117	5.117	10.920	50.334	35.334	
	OW	1.992	1.825	1.582	7.293	5.117	2.633
1-4 pairs	CH	1.665	1.665	3.551	3.736		
	CH2	2.297	2.297	4.899	5.155	7.113	
C_6		OA	O	C	CH	CH2	OW
general pairs	OA	2.262					
	O	2.262	2.262				
	C	2.301	2.301	2.340			
	CH	5.318	5.318	5.410	12.498		
	CH2	4.535	4.535	4.615	10.661	9.096	
	OW	2.433	2.433	2.475	5.720	4.879	2.617
1-4 pairs	CH	2.566	2.566	2.610	2.912		
	CH2	3.269	3.269	3.325	3.709	4.724	

[a] C_{12} parameters in GJ Å^{12} mol^{-1}. C_6 parameters in MJ Å^6 mol^{-1}.

TABLE 9

Parameters[a] of the potential functions governing the bonded interactions

Bonds (b)	k_b	b_0	*Improper dihedrals (θ)*	k_θ	θ_0	
HO-OA	3140	1.00	C-OA-CH-O, C-OA-CH2-O	167	0.0	
OA-C	3770	1.36	C_2-C_1-C_3-O_2	335	35.0	
OA-CH	3350	1.43				
O-C	5020	1.23	*Torsion angles (ϕ)*	k_ϕ	δ_ϕ	n_ϕ
CH-C, CH2-C, CH2-CH	3350	1.53				
			HO-OA-C-O	16.7	180.0	2
Angles (α)	k_α	α_0	CH-CH2-C-O	0.4	0.0	6
			C-CH2-CH-C (Ψ)	5.9	0.0	3
HO-OA-C, HO-OA-CH	397	109.5	H_2-O_2-C_2-C_1	5.6	180.0	1
OA-CH-C, OA-CH-CH2,			H_2-O_2-C_2-C_1	1.0	0.0	2
C-CH-CH2	460	109.5	H_2-O_2-C_2-C_1	2.0	0.0	3
C-CH2-CH	460	111.0	O_2-C_2-C_1-O_{1*}	0.1	0.0	1
OA-C-CH, OA-C-CH2	502	115.0	O_2-C_2-C_1-O_{1*}	9.4	180.0	2
O-C-CH, O-C-CH2	502	121.0	O_2-C_2-C_1-O_{1*}	3.3	180.0	3
OA-C-O	502	124.0				

[a]See the text for explanation of symbols. Bond lengths in Å. Angles in degrees. k_b in kJ mol^{-1} Å^{-2}. k_α and k_θ in kJ mol^{-1} degree^{-2}. k_ϕ in kJ mol^{-1}.

torsion angles and so called improper dihedrals. Improper dihedral potentials depend on hybridization and define the relative positions of substituents attached to one carbon. They keep the C–OA–CH/CH2–O groups, where C is the pivot to which the other atoms are attached, planar and also define the left-handed chirality of the C_2–C_1–C_3–O_2 group. Bonds, angles and improper dihedrals (denoted by λ) are subject to harmonic potential functions: $V_\lambda = \frac{1}{2} k_\lambda (\lambda - \lambda_0)^2$, where k_λ is the force constant and λ_0 defines the position of the minimum. Torsion angles ϕ obey sinusoidal functions $V_\phi = k_\phi (1 + \cos(n_\phi \times \phi - \delta_\phi))$, where n_ϕ is the multiplicity of the rotation (number of minima between 0 and 360°) and δ_ϕ defines the positions of the minima, since $n_\phi \times \phi_{min} - \delta_\phi = 180 \bmod 360°$. Parameters of bond, angle, torsion and improper dihedral potentials for malic acid are given in Table 9. Water, as mentioned, is completely rigid and has intramolecular OW–HW and HW–HW distances of 1.000 and 1.633 Å, respectively.

REFERENCES

1 P. van der Sluis and J. Kroon, Acta Crystallogr., Sect. C, 41 (1985) 956.
2 J.F.J. van Loock, W. van Havere and A.T.H. Lenstra. Bull. Soc. Chim. Belg., 90 (1981) 161.
3 J.S. Mariano and V.M.S. Gil. Mol. Phys., 17 (1969), 313.
4 L.M.J. Kroon-Batenburg, Thesis, Hydrogen Bonding and Molecular Conformation, State University of Utrecht, The Netherlands, 1985.
5 P.F.W. Stouten and J. Kroon, J. Mol. Struct., (1988) in press.

6 J. Lautz, H. Kessler, R. Boelens, R. Kaptein and W.F. van Gunsteren, Int. J. Peptide Protein Res., 30 (1987) 404.
7 W.F. van Gunsteren, H.J.C. Berendsen, J. Hermans, W.G.J. Hol and J.P.M. Postma, Proc. Natl. Acad. Sci. (USA), 80 (1983) 4315.
8 W.F. van Gunsteren and H.J.C. Berendsen, J. Computer Aided Mol. Design, 1 (1987) 171.
9 W.F. van Gunsteren, GROMOS86, Groningen Molecular Simulation computer program package, State University of Groningen, The Netherlands, 1986.
10 H.J.C. Berendsen, J.P.M. Postma, W.F. van Gunsteren and J. Hermans, in B. Pullman (Ed.), Intermolecular Forces, Reidel, Dordrecht, 1981, p. 331.
11 P.F.W. Stouten, L.M.J. Kroon-Batenburg and J. Kroon, to be published.
12 M.D. Newton and G.A. Jeffrey, J. Am. Chem. Soc., 99 (1977) 2413.
13 W.F. van Gunsteren and M. Karplus, Macromolecules, 15 (1982) 1528.
14 H.J.C. Berendsen, J.P.M. Postma, W.F. van Gunsteren, A. DiNola and J.R. Haak, J. Chem. Phys., 81 (1984) 3684.
15 T.P. Straatsma, H.J.C. Berendsen and A.J. Stam, Mol. Phys., 57 (1986) 89.
16 M. Karplus, J. Chem. Phys., 30 (1959) 11.
17 R.G. Bates, Determination of pH, Wiley New York, 1965[II], Ch. 8, p. 220.
18 P.K. Glasoe and F.A. Long. J. Phys. Chem., 64 (1960) 188.
19 G. Dahlgren Jr. and F.A. Long, J. Am. Chem. Soc., 82 (1960) 1303.
20 B.M. Lowe and D.G. Smith, J. Chem. Soc., Faraday Trans. 1, 70 (1974) 362.
21 R.C. Das, U.N. Dash and K.N. Panda, J. Chem. Soc., Faraday Trans. 1, 76 (1980) 2152.
22 R.A. Alberty and P. Bender, J. Am. Chem. Soc., 81 (1959) 542.
23 L.E. Erickson, J. Am. Chem. Soc., 87 (1965) 1867.
24 C.A.G. Haasnoot, F.A.A.M. de Leeuw and C. Altona, Tetrahedron, 36 (1980) 2783.
25 M.L. Huggins, J. Am. Chem. Soc., 75 (1953) 4123.
26 F.H. Allen, S. Bellard, M.D. Brice, B.A. Cartwright, A. Doubleday, H. Higgs, T. Hummelink, B.G. Hummelink-Peters, O. Kennard, W.D.S. Motherwell, J.R. Rogers and D.G. Watson. Acta Crystallogr., Sect. B, 35 (1979) 2331.